
Article:
Yang, H., Lyu, S., Lin, H. et al. (2018) A variable-mode stator consequent pole memory machine. AIP Advances, 8 (5). 056612. ISSN: 2158-3226

https://doi.org/10.1063/1.5007220

A variable-mode stator consequent pole memory machine

Hui Yang, Shukang Lyu, Heyun Lin, and Z. Q. Zhu

Citation: AIP Advances **8**, 056612 (2018); doi: 10.1063/1.5007220
View online: https://doi.org/10.1063/1.5007220
View Table of Contents: http://aip.scitation.org/toc/adv/8/5
Published by the American Institute of Physics

A variable-mode stator consequent pole memory machine

Hui Yang,[1,a] Shukang Lyu,[1] Heyun Lin,[1] and Z. Q. Zhu[2]
[1]*School of Electrical Engineering, Southeast University, Sipailou 2, 210096 Nanjing, China*
[2]*Department of Electronic and Electrical Engineering, University of Sheffield, Mappin Street, Sheffield S1 3JD, UK*

(Presented 7 November 2017; received 1 October 2017; accepted 28 October 2017; published online 14 December 2017)

In this paper, a variable-mode concept is proposed for the speed range extension of a stator-consequent-pole memory machine (SCPMM). An integrated permanent magnet (PM) and electrically excited control scheme is utilized to simplify the flux-weakening control instead of relatively complicated continuous PM magnetization control. Due to the nature of memory machine, the magnetization state of low coercive force (LCF) magnets can be easily changed by applying either a positive or negative current pulse. Therefore, the number of PM poles may be changed to satisfy the specific performance requirement under different speed ranges, i.e. the machine with all PM poles can offer high torque output while that with half PM poles provides wide constant power range. In addition, the SCPMM with non-magnetized PMs can be considered as a dual-three phase electrically excited reluctance machine, which can be fed by an open-winding based dual inverters that provide direct current (DC) bias excitation to further extend the speed range. The effectiveness of the proposed variable-mode operation for extending its operating region and improving the system reliability is verified by both finite element analysis (FEA) and experiments.
https://doi.org/10.1063/1.5007220

I. INTRODUCTION

Due to the urgent issues on environment preservation and energy conservation, electric vehicles (EVs) have experienced a significant growth in recent years. Memory machine (MM)[1,2] has been widely recognized as a potential candidate for EVs, which has the distinct synergies of acceptable torque capability in low-speed operation and good flux-weakening capability as well as high efficiency in high-speed operation. Very recently, numerous novel topologies of MMs have emerged, and a novel stator-consequent-pole memory machine (SCPMM)[3] was proposed to combine the advantages of simple rotor and easy manufacturability in doubly salient reluctance machine as well as excellent energy-efficient flux adjusting capability in MM. The topology of 6/7-pole SCPMM is shown in Fig. 1(a). Due to the use of low coercive force permanent magnets (PMs), aluminum-nickel-cobalt (Al-Ni-Co), the airgap flux density of the machine can be regulated online by changing the magnetizing state of PMs. However, it is relatively hard to perform the magnetization control precisely and continuously. Therefore, the "pole-changing" concept[4] is applied to SCPMM. In this way, parts of PMs can be fully demagnetized to implement the flux-weakening control. It is worth noting that when all the PMs are fully demagnetized, the SCPMM is similar to a variable flux reluctance machine (VFRM).[5,6] Thus, it is practical to further utilize a dual-three phase inverter to generate the zero-sequence current to achieve the electrically excited operation. The purpose of this paper is to realize the coordinated control for SCPMM when it works with all PM poles, half PM poles and zero PM pole, respectively. All the three modes will be synthesized to extend the speed range and improve the system reliability. The main design parameters of the prototype SCPMM are listed in Table I.

[a]huiyang@seu.edu.cn.

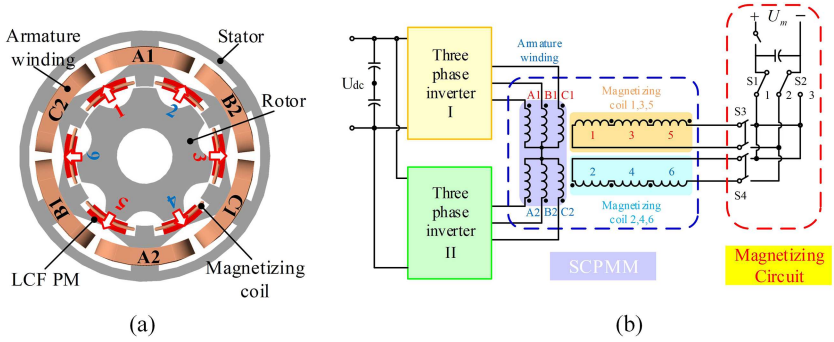

FIG. 1. (a) The topology of the proposed SCPMM. (b) The illustration of the variable-mode control circuit.

TABLE I. Parameters of the prototype SCPMM.

Parameter	Value	Parameter	Value
Stator outer diameter (mm)	100	PM thickness (mm)	6.25
Stator inner diameter (mm)	55	PM width (mm)	7.5
Air-gap length (mm)	0.50	Magnet grade	Al-Ni-Co 140
Active stack length (mm)	80	Steel sheet grade	50CS350

II. WINDING CONFIGURATION

The winding configuration enabling the variable-mode operation is presented in Fig. 1(b), which consists of a dual-three phase inverter with a single voltage source and a magnetizing control circuit. When the SCPMM works in the electrically excited mode, the zero-sequence current for the direct current (DC) excitation can be generated through the dual-three phase inverter with the single voltage source. Meanwhile, in the magnetizing control circuit, the six magnetizing coils can be separated into two groups where coils 1, 3, 5 and coils 2, 4, 6 are connected in series, respectively. At the beginning of the magnetizing or demagnetizing process, the DC voltage source charges the capacitor and then turns off switch S5. The capacitor produces positive or negative current pulse depending on the states of switches S1, S2, S3 and S4, which can decide whether the two coil groups receive the current pulse. Therefore, the PMs can be either fully magnetized or demagnetized through the magnetizing control circuit.

III. PERFORMANCE OF VARIABLE MODE OPERATION FOR SCPMM

A. Electromagnetic characteristic analysis

Firstly, in order to illustrate the electromagnetic characteristic of the variable-mode SCPMM explicitly, the PM excitation mode and the electrically excited mode will be discussed separately. Fig. 2 shows the open circuit magnetic fields of SCPMM in different modes. From Fig. 2(a), the SCPMM works at flux-enhanced mode when all the six PMs are fully magnetized in the same directions, producing relatively high torque output. If half PM poles are fully demagnetized, the magnetic field is weakened as shown in Fig. 2(b) so that the attainable maximum speed of SCPMM can be increased. Fig. 2(c) shows the flux density distribution of the SCPMM in the electrically excited mode and the airgap magnetic field can be adjusted simply through regulating the excitation current when all the PMs are fully demagnetized. In these cases, the excitation current control will be utilized to further extend the machine speed range. Meanwhile, the electrically excited mode is able to serve as an alternate mode to improve the system reliability.

Figs. 3(a) and 3(b) show the radial air-gap flux density distributions and the corresponding harmonic spectra of the SCPMM in different modes where "*Zs*" presents the number of stator slots and "*Zr*" indicates the number of rotor slots. It can be observed that the amplitudes of dominant

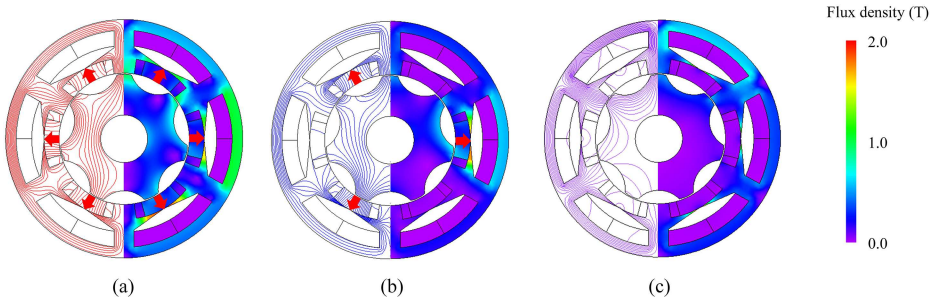

FIG. 2. Open circuit flux lines of SCPMM in different modes. (a) SCPMM with all PM poles. (b) SCPMM with half PM poles. (c) SCPMM without PMs and when the excitation current is 2.5A.

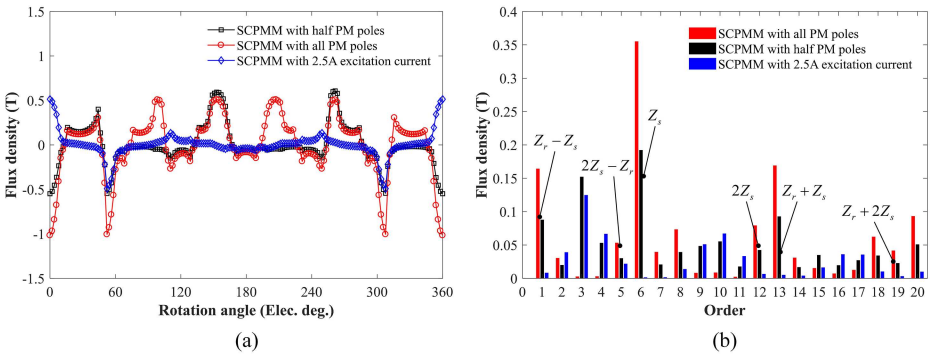

FIG. 3. (a) No-load radial air-gap flux density waveforms. (b) The harmonic spectra of air gap flux densities in different modes.

harmonic components are basically halved when the machine switches from the all PM poles mode to the half PM poles mode. In addition, when the machine operates at the electrically excited mode, the magnitudes of flux density vary proportionally with the value of excitation current. In Fig. 3(b), the working harmonic components of the machine with 2.5A excitation current are further reduced compared to those with the PM excitation so that the wider speed range can be obtained in the electrically excited mode due to better flux-weakening effect.

B. Torque-speed curves under variable-mode operation

The main target of the variable-mode operation is to extend the operation region of the SCPMM. The flux linkage method[7] is utilized to predict the torque-speed curve of the machine in different modes and it shows better computation speed compared to the direct FE method albeit with the comparable accuracy due to the consideration of cross coupling effect.

The electromagnetic torque of the SCPMM can be expressed as

$$T = \frac{3}{2} p[\psi_d(i_d, i_q) i_q - \psi_q(i_d, i_q) i_d] \tag{1}$$

where p is the rotor pole number; ψ_d and ψ_q are the d- and q-axis flux linkages, respectively; i_d and i_q are the d- and q-axis currents, respectively.

When the SCPMM works in flux-weakening region, the applied voltage and current will be limited by the maximum voltage u_{max} and current i_{max} which can be described as

$$\begin{cases} u = \sqrt{u_d^2 + u_q^2} = \sqrt{(Ri_d - \omega\psi_q(i_d, i_q))^2 + (Ri_q + \omega\psi_d(i_d, i_q))^2} \le u_{\max} \\ i = \sqrt{i_d^2 + i_q^2} \le i_{\max} \end{cases} \tag{2}$$

where R is the phase resistance, ω is the electrical angular velocity, u is the phase voltage and i is the phase current, u_d and u_q are the d- and q-axis voltages, respectively.

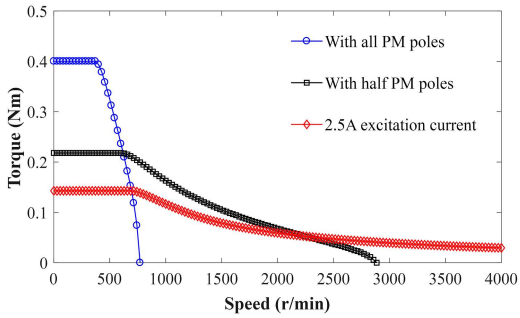

FIG. 4. Torque-speed characteristic comparison of SCPMM in different modes.

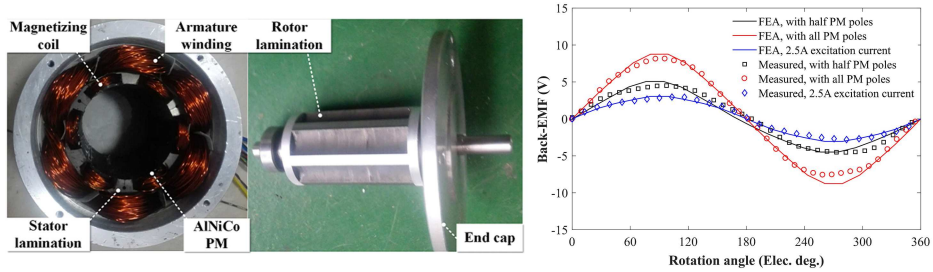

(a) (b)

FIG. 5. (a) Prototype machine. (b) Test back-EMFs of SCPMMs in different modes.

After acquiring the 3-D look up tables of $\psi_d(i_d, i_q)$ and $\psi_d(i_d, i_q)$ by FE method which can take the cross coupling effect into consideration, the torque-speed characteristics of the SCPMM at different modes can be calculated as shown in Fig. 4. According to Fig. 4, a high torque output can be provided when the machine is in low speed operation, while the speed range can be further extended in the cases of the half PM poles mode and electrically excited mode. Therefore, it is practical to combine the three operating modes to extend the working region of the SCPMM.

IV. EXPERIMENT

A SCPMM prototype with 6 stator slots and 7 rotor salient poles is fabricated as shown in Fig. 5(a). The measured open-circuit back-electromotive force (EMF) of the prototype machine in different modes are shown in Fig. 5(b). According to Fig. 5(b), the back-EMF magnitude of SCPMM with half PM poles is almost half that with all PM poles. In addition, the back-EMF amplitude of SCPMM with only 2.5A electric excitation current is much lower than those with PM excitations, which confirms the feasibility of the variable-mode operation for effective flux-weakening. The variable-mode control circuit is under construction, and the further experimental results will be reported in the future papers.

V. CONCLUSION

A variable-mode concept is proposed for a SCPMM for the global flux-weakening in this paper. In addition, the electrically excited mode can serve as an alternate mode to improve the system reliability. A flux linkage method is utilized to accurately predict the torque-speed characteristic of the machine in different modes, which can take the cross-coupling effect into consideration. It is confirmed that the three operating modes can be combined to extend the working region of the machine. The effectiveness of the variable-mode operation is validated by both finite element prediction and experimental measurement. For the further work, it is necessary to evaluate the efficiency of the variable-mode SCPMM in the whole working range.

ACKNOWLEDGMENTS

This work was jointly supported by National Natural Science Foundation of China (51707036 and 51377020), Specialized Research Fund for the Doctoral Program of Higher Education of China (20130092130005), Natural Science Foundation of Jiangsu Province for Youth (BK20170674), and the Fundamental Research Funds for the Central Universities (3216007453).

[1] V. Ostovic, IEEE Ind. Appl. Mag. **9**, 52 (2003).
[2] C. Yu and K. T. Chau, IEEE Trans. Ind. Appl. **47**, 2031 (2011).
[3] H. Yang, H. Lin, Z. Q. Zhu, S. Fang, and Y. Huang, in 2016 IEEE Energy Convers. Congr. and Expo. (ECCE), Milwaukee, USA, 2016, pp. 1–8.
[4] T. Niizuma and K. Sakai, in Int. Conf. Electr. Mach. Syst. (ICEMS), Sapporo, Japan, 2012, pp. 1–4.
[5] Z. Q. Zhu and B. Lee, IEEE Trans. Energy Convers. **32**, 447 (2017).
[6] Z. Q. Zhu, B. Lee, and X. Liu, IEEE Trans. on Ind. Appl. **52**, 1519 (2016).
[7] G. Qi, J. T. Chen, Z. Q. Zhu, D. Howe, L. B. Zhou, and C. L. Gu, IEEE Trans. Magn. **45**, 2110 (2009).